Supplementary Materials

Model description

The *ecosys* model has been rigorously examined in many high-latitude ecosystems, e.g.: modeled energy and carbon fluxes against data from eddy covariance flux towers at the Barrow Experimental Observatory (BEO) (Grant *et al* 2017b, 2017a) and a topographic gradient at Daring Lake, NWT (Grant 2015a, Grant *et al* 2015) , and against long-term measurements from automated chambers in the Stordalen Mire(Chang *et al* 2019, n.d.). The model performance has also been tested and documented in sites from many biomes encompassing a range of latitudes in a long list of *ecosys* publications (5-92). The following qualitative model description is adapted from our earlier publication.

Ecosys represents multiple canopy and soil layers and fully coupled carbon, energy, water, and nutrient cycles solved at an hourly time step. Surface energy and water exchanges drive soil heat and water transfers to determine soil temperatures and water contents. These transfers drive soil freezing and thawing and, hence, active layer depth, through the general heat flux equation. Carbon uptake is controlled by plant water status calculated from convergence solutions that equilibrate total root water uptake with transpiration. Atmospheric warming increases surface heat advection, soil heat transfers, and hence active layer depth. Canopy temperatures affect CO_2 fixation rates from their effects on carboxylation and oxygenation modeled with Arrhenius functions for light and dark reactions. Soil temperatures affect heterotrophic respiration through the same Arrhenius function as for dark reactions.

Carbon uptake is also affected by plant nitrogen uptake. The model represents fully coupled transformations of soil carbon, nitrogen, and phosphorus through microbially driven processes. Soil warming enhances carbon uptake by hastening microbial mineralization and root nitrogen uptake. Carbon uptake is affected by phenology with leafout and leafoff (deciduous plants) or dehardening and hardening (evergreen plants) being determined by accumulated exposure to temperatures above set values while day length is increasing or below set values while day length is decreasing. Senescence is driven by excess maintenance respiration and by phenology in deciduous plant functional types.

Ecosystem-Atmosphere energy exchange:

Canopy energy and water exchanges in *ecosys* are calculated through a multi-layered soil-root-canopy system. The clumping effect for each leaf and stem surface is represented by a species-specific interception fraction to simulate non-uniformity in the horizontal distribution of leaves within each canopy layer. Coupled first-order closure schemes are solved between the atmosphere and each of leaf and stem surfaces in the multi-layered canopy to achieve energy balance at each model time step. Once the system converges to the required canopy temperature, latent and sensible heat fluxes of each canopy layer are calculated based on the simulated vapor pressure deficit, canopy-atmosphere temperature gradient, aerodynamic conductance, and stomatal conductance. Canopy heat storage is calculated from changes in canopy temperature and heat capacities of leaves, twigs, and stems.

Canopy water relations:

A convergence solution is sought for the canopy water potential of each plant population at which the difference between its transpiration and total root water uptake equals the difference between its water contents at the previous and current water potentials. Canopy water potential controls transpiration and soil-root water uptake, which affects stomatal conductance and thereby all the processes (e.g., canopy temperature and vapor pressure) described in "Ecosystem-Atmosphere energy exchange". The water table depth in *ecosys* is calculated at the end of each time step as the depth to the top of the saturated zone below which air-filled porosity is zero. Changes in the simulated water table depth were driven by dynamical interactions among precipitation, evapotranspiration, vertical water transport, and lateral water transport.

Canopy carbon and nutrient cycling:

Leaf carboxylation rates are adjusted from those calculated under non-limiting water potential to those under current water potential. The gross canopy CO_2 fixation is the sum of the leaf carboxylation rate of each leaf surface present on each branch of each plant species, which is then transported to a mobile pool of carbon storage. Storage carbon oxidized in excess of maintenance respiration requirements is used as growth respiration to drive the formation of new biomass. Net CO_2 fixation is calculated as the difference between gross fixation and the sum of maintenance, growth, and senescence respiration in the simulated canopy.

Nutrient (nitrogen and phosphorous) uptake is calculated for each plant species by solving for aqueous concentrations at root and mycorrhizal surfaces in each soil layer at which radial transport by mass flow and diffusion from the soil solution to the surfaces equals active uptake by the surfaces. This solution dynamically links rates of soil nutrient transformations with those of root and mycorrhizal nutrient uptake. The products of nitrogen and phosphorous uptake are transported to mobile pools of nitrogen and phosphorous stored in each root and mycorrhizal layer, which regulate vegetation growth.

Plant functional type dynamics:

The model represents prognostic vegetation dynamics with internal resource allocation and remobilization. Shifts in plant functional types are modeled through processes of plant functional type competition for light, water, and nutrients within each canopy and rooted soil layer depending on leaf area and root length. Each plant functional type competes for nutrient and water uptake from common nutrient and water stocks held across multi-layer soil profiles, calculated from algorithms for transformations and transfers of soil carbon, nitrogen, and phosphorus, and for transfers of soil water. Modeled differences in plant functional type functional traits determine the strategy of resource acquisition and allocation that drive growth, resource remobilization, and litterfall, and therefore each plant functional type dynamic competitive capacity under different environmental conditions.

Soil microbial activity:

The modeling of microbial activity is based on six organic states: solid, soluble, sorbed, acetate, microbial biomass, and microbial residues. Carbon, nitrogen and phosphorous may move among these states within each of four organic matter-microbe complexes: plant litterfall, animal manure, particulate organic matter, and humus. Microbial biomass in *ecosys* is an active agent of organic matter transformation. The rate at which each component is hydrolyzed is a function of substrate concentration that approaches a first-order function at low concentrations, and a zero-order function at high concentrations. These rates are regulated by soil temperature through an Arrhenius function and by soil water content through its effect on substrate concentration. Similar to the growth and decline of vegetation biomass described above, the net change in microbial biomass is determined by the difference between heterotrophic respiration and maintenance

respiration. When heterotrophic respiration is greater than maintenance respiration, the excessive amount of respiration is used as growth respiration that drives microbial growth according to the energy requirements of biosynthesis.

Methane production and transport:

The rate at which soil organic matter in *ecosys* is hydrolyzed during decomposition is a first-order function of the decomposer biomass of all heterotrophic microbial populations (functional types) generated from energy yields of the oxidation-reduction reactions conducted by each population. Hydrolysis rates are regulated by soil temperature through an Arrhenius function and by soil water content through its effect on aqueous microbial concentrations. Hydrolysis products are transferred to dissolved organic carbon (DOC) that is the substrate for respiration and growth according to energy yields from DOC oxidation-reduction by all heterotrophic microbial functional types (MFT) calculated from MFT biomass, a Michaelis-Menten function of DOC concentration, and from soil temperature and oxygen availability. DOC uptake by anaerobic MFTs (fermenters) drives fermentation products of which are partitioned among acetate (CH_3COOH), CO_2, and hydrogen (H_2) according to Brock & Madigan (1991). These products are substrates for acetoclastic (AM) and hydrogenotrophic methanogenesis (HM), rates of which are driven by biomasses of AM and HM functional types, growths of which are generated from AM and HM energy yields. For all MFTs, respiration products beyond those used for microbial maintenance respiration drives microbial growth. Specifically, AM (HM) microbial growth is calculated by dividing the free energy change of AM (HM) by the energy required to construct new AM (HM) microbial carbon, which drives changes in AM (HM) microbial biomass after subtracting biomass loss from decomposition. CH_4 production rates are functions of microbial biomass, temperature, substrate concentrations, and moisture for AM and HM MFTs in each model soil layer during each hourly model time step. CH_4 produced by AM and HM can then be transported to the atmosphere through diffusion, plant aerenchyma transport, and ebullition, or oxidized by methanotrophs. Detailed equation sets for methanogenesis and methanotrophy used in *ecosys* were derived in Grant, (1998; 1999) and remain unchanged in other studies of methanogenesis (e.g. Grant et al., 2017, 2019) since then.

Supplementary Table 1. Evaluation of modeled apparent CH_4 emission temperature dependence calculated by fitting Boltzmann-Arrhenius functions with soil and air temperatures during the earlier, later, and full-season (entire thawed season) periods in the bog and fen at the Stordalen Mire.

	Soil temperature				Air temperature			
2003-2007								
	Earlier		Later		Earlier		Later	
	hysteretic	full-season	hysteretic	full-season	hysteretic	full-season	hysteretic	full-season
	R^2				R^2			
Bog	0.68	0.62	0.49	0.31	0.40	0.32	0.36	0.05
Fen	0.84	-0.95	0.71	-0.93	0.11	-0.18	0.14	-0.24
	RMSE				RMSE			
Bog	10.75	11.68	14.93	17.34	13.39	14.22	17.07	20.92
Fen	10.43	36.06	23.49	60.86	44.65	51.37	53.69	64.51
	Percent error				Percent error			
Bog	-3.95	10.29	-3.02	-21.01	-14.20	20.48	-12.81	-51.17
Fen	-2.45	81.22	-1.37	-40.35	-15.07	36.97	-8.02	-57.64
	E_a				E_a			
Bog	1.88	1.82	1.49	1.78	1.47	1.25	1.17	1.23
Fen	1.34	0.98	0.42	0.97	1.57	1.25	1.17	1.27
2011-2013								
	R^2				R^2			
Bog	0.73	0.59	0.61	0.17	-1.34	-2.69	0.30	-0.17
Fen	0.86	0.01	0.76	-1.12	-0.12	-1.19	0.20	-0.55
	RMSE				RMSE			
Bog	8.72	10.81	10.60	15.57	17.88	22.47	17.42	22.63
Fen	29.21	76.88	39.50	119.42	90.78	126.80	112.14	156.44
	Percent error				Percent error			
Bog	-2.88	16.39	-1.92	-21.48	-0.93	56.28	-10.08	-38.17
Fen	-2.61	71.76	-0.53	-34.25	-22.90	61.11	-11.11	-52.16
	E_a				E_a			
Bog	1.85	1.58	1.16	1.61	2.18	1.66	1.07	1.65
Fen	1.21	1.04	0.45	1.05	1.91	1.53	1.10	1.61

R^2, RMSE, and E_a are the correlation, root mean squared error (in mg C m^{-2} d^{-1}), and activation energy (in eV), respectively, from fitting Eq. 1 to the *ecosys*-modeled fluxes. Negative R^2 implies the regression line fitted by Boltzmann-Arrhenius functions is worse than using the mean value.

Supplementary Table 2. Evaluation of modeled apparent CH_4 emission temperature dependence calculated by fitting Boltzmann-Arrhenius functions with soil and air temperatures during the earlier, later, and full-season (entire thawed season) periods in the trough, rim, center, and polygon mean in a low-centered polygon at Utqiaġvik (formerly Barrow) in 2013.

	Soil temperature				Air temperature			
	Earlier		Later		Earlier		Later	
	hysteretic	full-season	hysteretic	full-season	hysteretic	full-season	hysteretic	full-season
	R^2				R^2			
Trough	0.44	0.07	0.25	-0.67	0.18	0.15	-0.04	-1.03
Rim	-0.11	-0.29	-0.69	-0.33	-0.20	-0.34	-0.47	-0.42
Center	0.58	0.04	0.52	-1.41	0.25	-0.08	0.11	-1.75
Polygon mean	0.60	0.06	0.42	-0.95	0.28	-0.13	0.08	-1.14
	RMSE				RMSE			
Trough	8.14	9.40	20.79	27.91	10.13	10.28	21.74	30.36
Rim	3.90	4.20	10.04	8.88	4.33	4.57	9.55	9.40
Center	13.24	19.98	13.58	30.52	17.68	21.19	18.84	33.12
Polygon mean	7.24	11.11	12.14	22.30	9.63	12.04	15.40	23.54
	Percent error				Percent error			
Trough	-22.59	50.02	-5.98	-64.31	-31.66	32.49	-16.14	-61.37
Rim	-27.87	-22.98	-43.55	-61.62	-30.95	-32.81	-57.49	-61.29
Center	-5.46	40.77	-1.81	-38.38	-12.40	29.73	-3.43	-37.15
Polygon mean	-5.77	45.40	-3.40	-44.45	-11.92	34.22	-6.15	-40.76
	E_a				E_a			
Trough	2.55	1.56	1.91	1.56	1.18	0.62	0.86	0.62
Rim	0.26	1.56	2.92	1.56	0.00	0.76	1.41	0.76
Center	1.75	0.71	0.67	0.71	0.78	0.28	0.25	0.28
Polygon mean	1.69	0.86	0.88	0.86	0.79	0.33	0.37	0.33

R^2, RMSE, and E_a are the correlation, root mean squared error (in mg C m^{-2} d^{-1}), and activation energy (in eV), respectively, from fitting Eq. 1 to the *ecosys*-modeled fluxes. Negative R^2 implies the regression line fitted by Boltzmann-Arrhenius functions is worse than using the mean value.

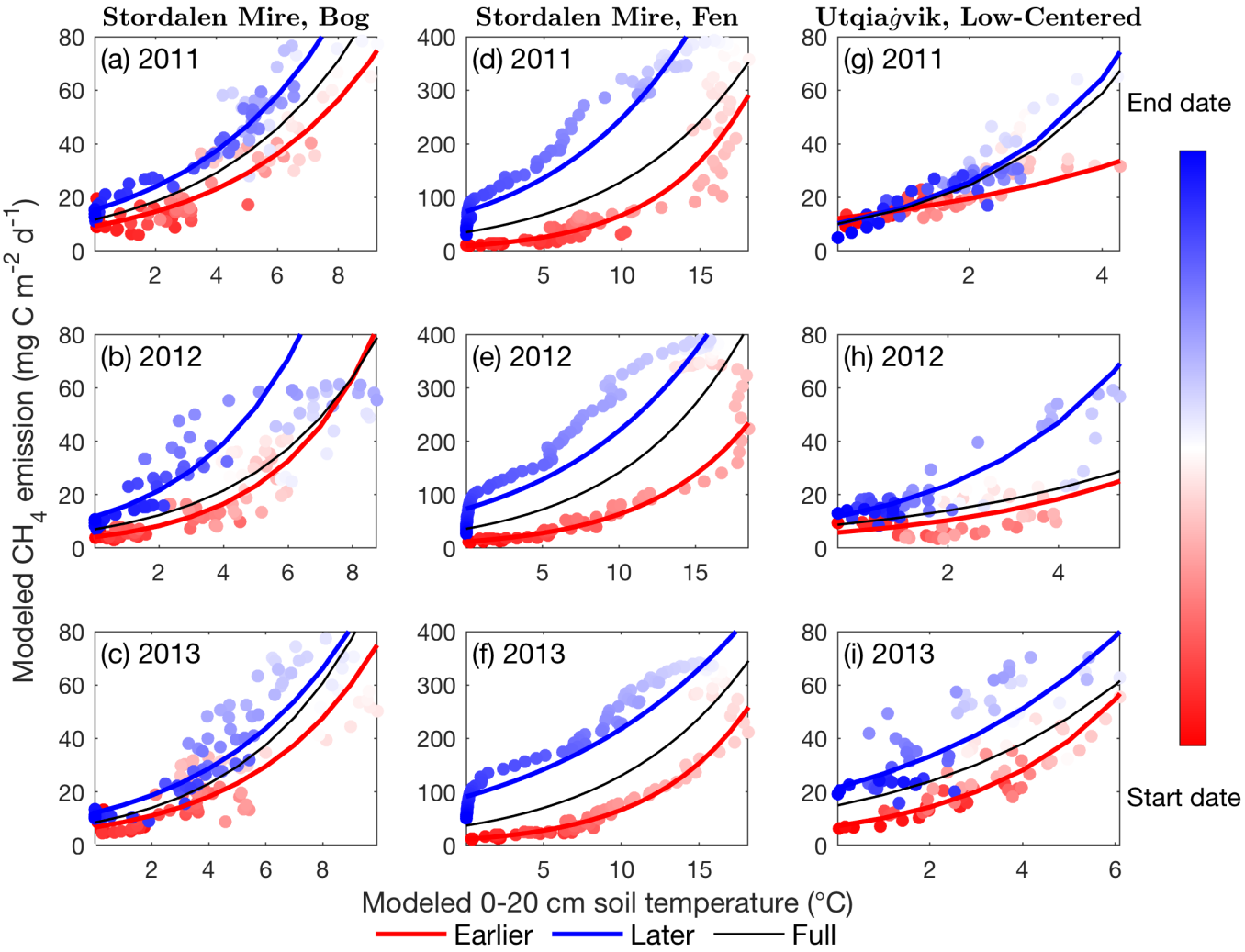

Supplementary Figure 1. CH_4 emissions are hysteretic to soil temperature modeled in the Stordalen Mire bog (a to c) and fen (d to f) and the Utqiaġvik low-centered polygon (g to i) from 2011 to 2013 thawed seasons. Dots and lines represent the daily data points and the fitted apparent temperature dependence, respectively. Earlier, later, and full-season periods are colored in red, blue, and black, respectively. Earlier and later periods are defined as the time before and after the seasonal maximum 0-20 cm soil temperature. Start date and end dates represent the beginning and ending of a thawed season defined as the period when daily 0-20 cm soil temperature is above 0 ˚C, respectively.

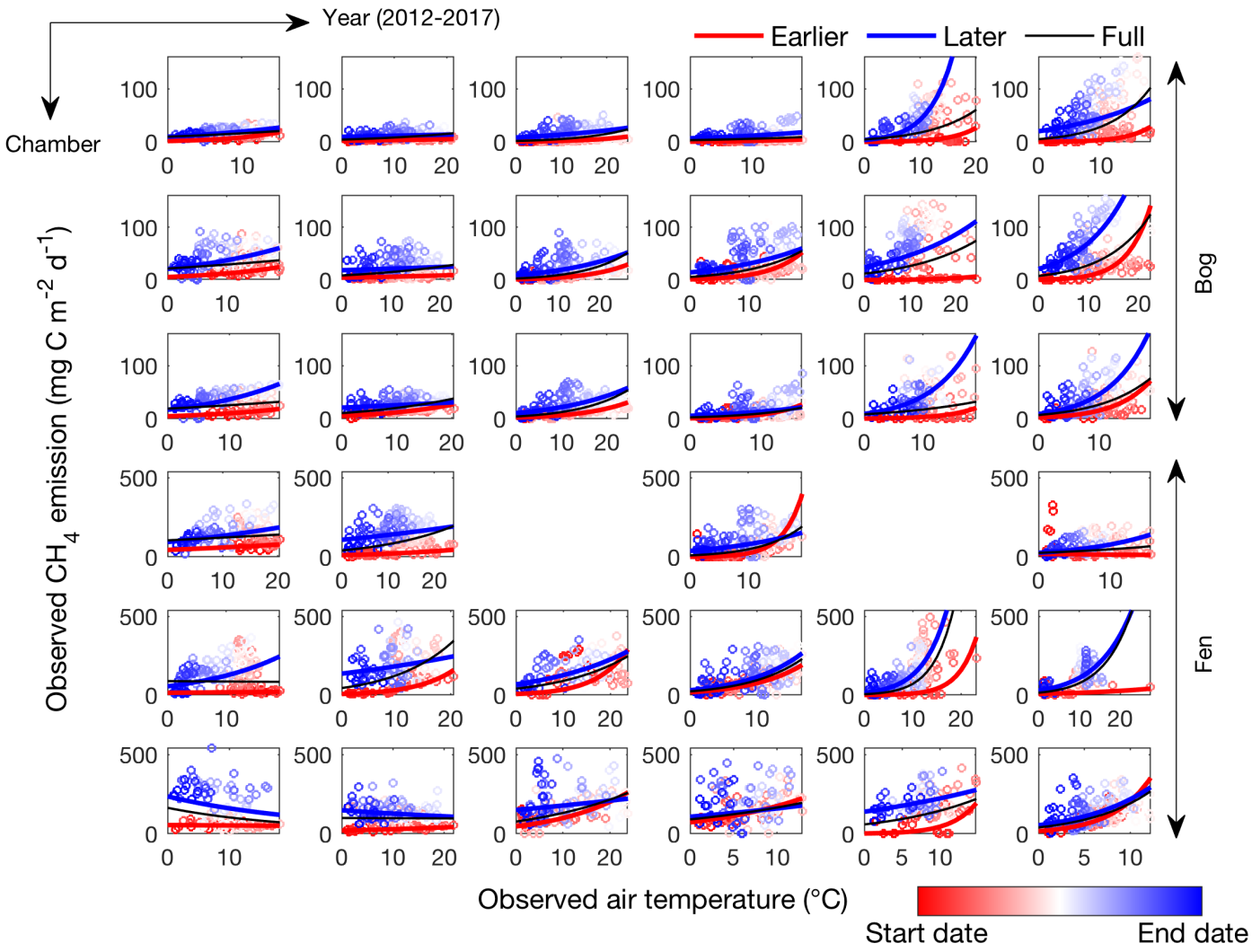

Supplementary Figure 2. CH_4 emissions are hysteretic to air temperature measured in individual automated chambers in the Stordalen Mire bog (top three panels) and fen (bottom three panels) sites from 2012 to 2017 thawed seasons (left to right). Open circles and lines represent the daily data points and the fitted apparent CH_4 emission temperature dependence, respectively. The earlier, later, and full-season periods are colored in red, blue, and black, respectively. Earlier and later periods are defined as the time before and after the seasonal maximum air temperature. Start date and end dates represent the beginning and ending of a thawed season defined as the period when daily air temperature is above 1 ˚C, respectively.

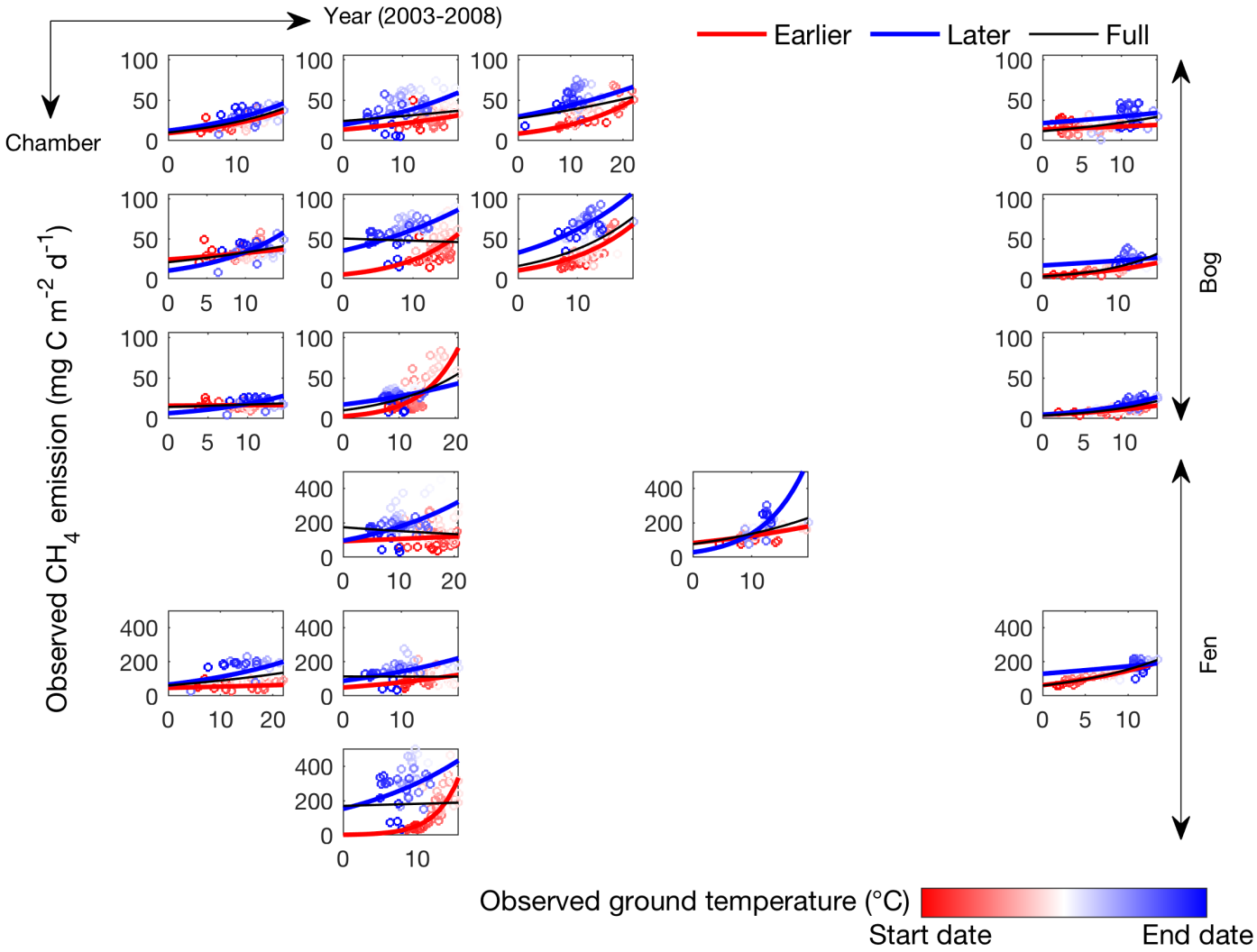

Supplementary Figure 3. CH_4 emissions are hysteretic to ground surface temperature measured in individual automated chambers in the Stordalen Mire bog (top three panels) and fen (bottom three panels) sites from 2003 to 2008 thawed seasons (left to right). Open circles and lines represent the daily data points and the fitted apparent CH_4 emission temperature dependence, respectively. The earlier, later, and full-season periods are colored in red, blue, and black, respectively. Earlier and later periods are defined as the time before and after the seasonal maximum ground surface temperature. Start date and end dates represent the beginning and ending of a thawed season defined as the period when daily ground surface temperature is above 1 ˚C, respectively.

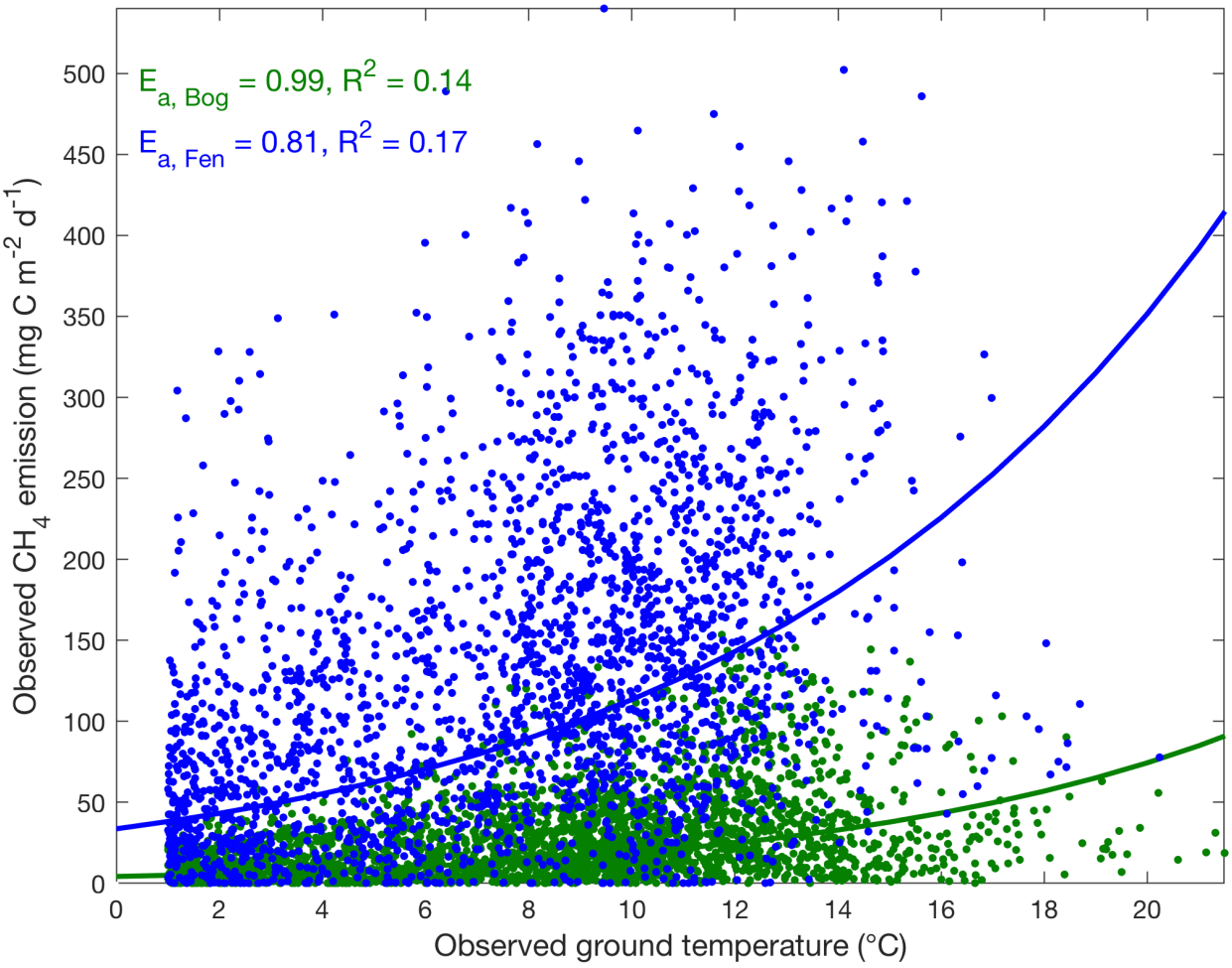

Supplementary Figure 4. Observed apparent relationships between thawed-season CH_4 emissions and ground temperature measured in the Stordalen Mire bog (green) and fen (blue) sites from 2012 to 2017, when spatial heterogeneity (i.e., differences across chambers within the same habitat) and temporal variability (i.e., intra-seasonal and inter-annual variations) are ignored. Dots and lines represent the daily data points and the fitted apparent CH_4 emission temperature dependence, respectively.

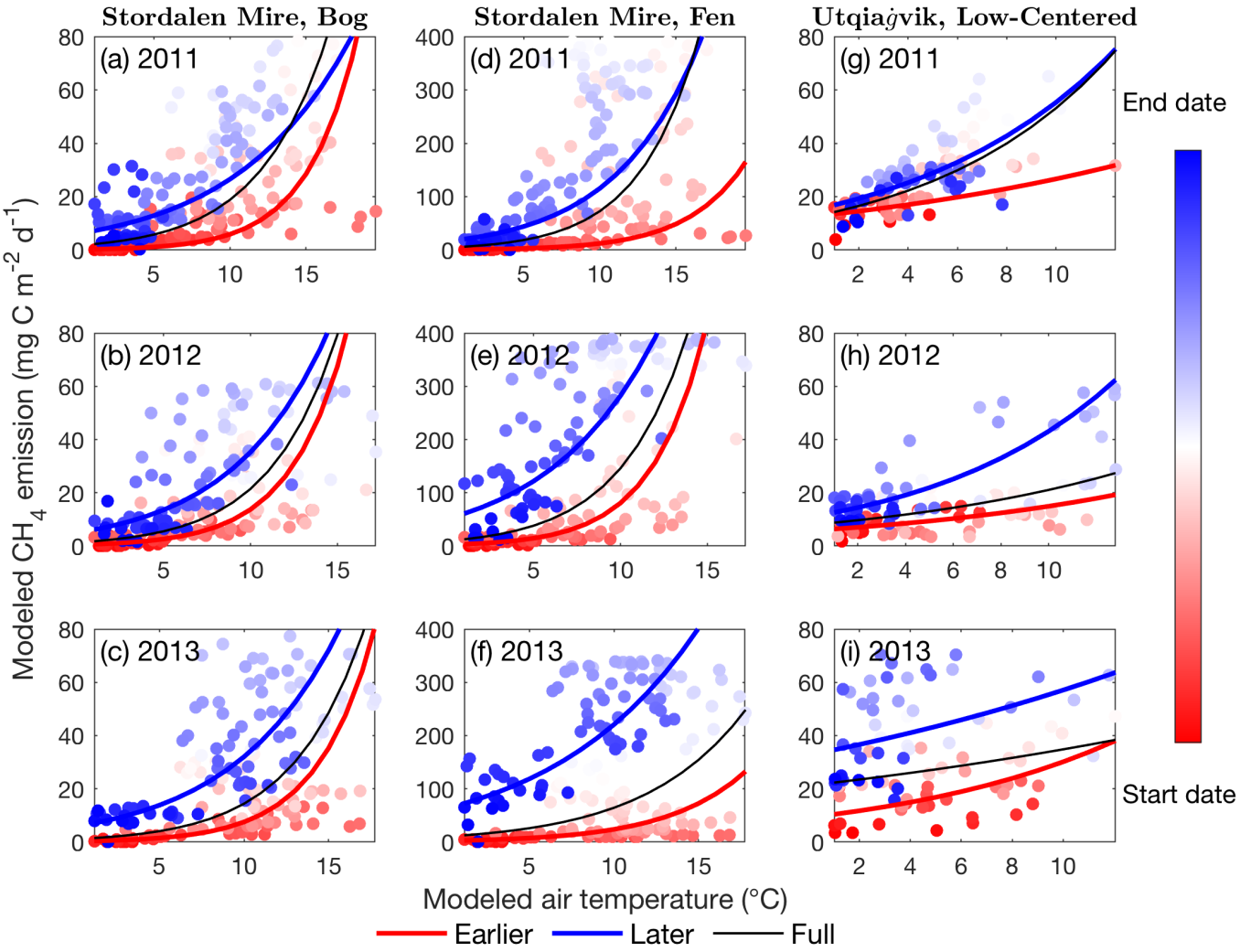

Supplementary Figure 5. CH_4 emissions are hysteretic to air temperature modeled in the Stordalen Mire bog (a to c) and fen (d to f) and the Utqiaġvik low-centered polygon (g to i) from 2011 to 2013 thawed seasons. Dots and lines represent the daily data points and the fitted apparent temperature dependence, respectively. Earlier, later, and full-season periods are colored in red, blue, and black, respectively. Earlier and later periods are defined as the time before and after the seasonal maximum air temperature. Start date and end dates represent the beginning and ending of a thawed season defined as the period when daily air temperature is above 1 ˚C, respectively.

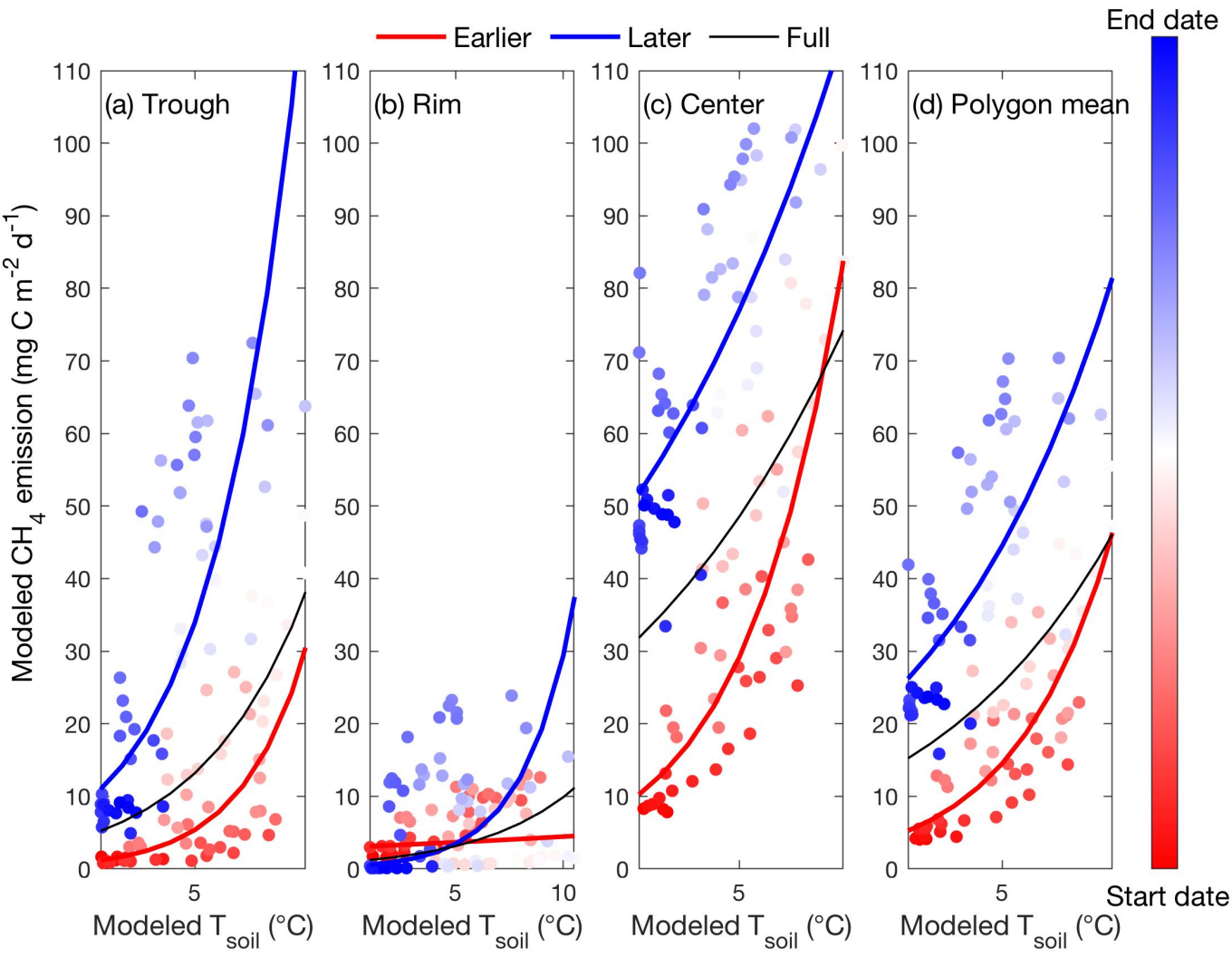

Supplementary Figure 6. Apparent soil temperature dependence of daily CH_4 emissions modeled in the trough (a), rim (b), center (c), and polygon mean (i.e., areal means of trough, rim, and center) (d) in a low-centered polygon at Utqiaġvik, Alaska during the 2013 thawed season. Dots and lines represent the daily data points and the fitted apparent temperature dependence, respectively. The earlier, later, and full-season periods are colored in red, blue, and black, respectively. Earlier and later periods are defined as the time before and after the modeled maximum 0-20 cm soil temperature. Start date and end dates represent the beginning and ending of a thawed season defined as the period when daily 0-20 cm soil temperature is above 1 ˚C, respectively. The hysteresis is less clear in the rim due to lower CH_4 emissions because of its drier conditions.

Reference:

Amthor J S, Chen J M, Clein J S, Frolking S E, Goulden M L, Grant R F, Kimball J S, King A W, McGuire A D, Nikolov N T, Potter C S, Wang S and Wofsy S C 2001 Boreal forest CO2 exchange and evapotranspiration predicted by nine ecosystem process models: Intermodel comparisons and relationships to field measurements *J. Geophys. Res. Atmos.*

Brock T D and Madigan M T 1991 *Biology of Microorganisms* (Prentice Hall, NJ)

Chang K-Y, Riley W J, Crill P M, Grant R F, Rich V I and Saleska S R 2019 Large carbon cycle sensitivities to climate across a permafrost thaw gradient in subarctic Sweden *Cryosph.* **13** 647–63 Online: https://www.the-cryosphere.net/13/647/2019/

Chang K-Y, Riley W J, McCalley C K, Crill P M, Grant R F and Brodie E L Methane production pathway regulated proximally by substrate availability and distally by temperature in a high-latitude mire complex

Dimitrov D D, Grant R F, Lafleur P M and Humphreys E R 2010a Modeling Peat Thermal Regime of an Ombrotrophic Peatland with Hummock–Hollow Microtopography *Soil Sci. Soc. Am. J.*

Dimitrov D D, Grant R F, Lafleur P M and Humphreys E R 2010b Modeling the Subsurface Hydrology of Mer Bleue Bog *Soil Sci. Soc. Am. J.* **74** 680 Online: https://www.soils.org/publications/sssaj/abstracts/74/2/680

Grant, F. R., Hesketh J D 1992 Canopy structure of maize (ZEA MA YS L.) AT at different populations: simulation and experimental verification *Biotronics* **21** 11–24

Grant R 2010 A Review of the Canadian Ecosystem Model — ecosys *Modeling Carbon and Nitrogen Dynamics for Soil Management*

Grant R 1994 Simulation of competition between barley and wild oats under different managements and climates *Ecol. Modell.*

Grant R . 1995 Mathematical modelling of nitrous oxide evolution during nitrification.pdf *Soil Biol. Biochem.* **27** 1117–25

Grant R F 2001a A Review of Canadian Ecosystem Model - ecosys *Model. Carbon Nitrogen Dyn. Soil Manag.* 173–264

Grant R F 1991a A Technique for Estimating Denitrification Rates at Different Soil Temperatures, Water

Contents, and Nitrate Concentrations *Soil Sci.* **152** 41–52

Grant R F 2015a Ecosystem CO 2 and CH 4 exchange in a mixed tundra and a fen within a hydrologically diverse Arctic landscape: 2. Modeled impacts of climate change *J. Geophys. Res. Biogeosciences* **120** 1388–406 Online: http://doi.wiley.com/10.1002/2014JG002889

Grant R F 2015b Ecosystem CO_2 and CH_4 exchange in a mixed tundra and a fen within a hydrologically diverse Arctic landscape: 2. Modeled impacts of climate change *J. Geophys. Res. Biogeosciences* **120** 1388–406 Online: http://doi.wiley.com/10.1002/2014JG002889

Grant R F 2004 Modeling topographic effects on net ecosystem productivity of boreal black spruce forests *Tree Physiol.* **24** 1–18

Grant R F 2001b Modeling Transformations of Soil Organic Carbon and Nitrogen at Differing Scales of Complexity *Model. Carbon Nitrogen Dyn. Soil Manag.* 672

Grant R F 2013 Modelling changes in nitrogen cycling to sustain increases in forest productivity under elevated atmospheric CO2 and contrasting site conditions *Biogeosciences* **10** 7703–21

Grant R F 2014 Nitrogen mineralization drives the response of forest productivity to soil warming: Modelling in ecosys vs. measurements from the Harvard soil heating experiment *Ecol. Modell.* **288** 38–46 Online: http://dx.doi.org/10.1016/j.ecolmodel.2014.05.015

Grant R F 1998a Simulation in ecosys of root growth reponse to contrasting soil water and nitrogen *Ecol.Model.* **107** 237–64

Grant R F 1998b Simulation in ecosys of root growth response to contrasting soil water and nitrogen *Ecol. Modell.*

Grant R F 1993 Simulation model of soil compaction and root growth - I. Model structure *Plant Soil*

Grant R F 1998c Simulation of methanogenesis in the mathematical model ecosys *Soil Biol. Biochem.* **30** 883–96

Grant R F 1999 Simulation of methanotrophy in the mathematical model ecosys *Soil Biol. Biochem.* **31** 287–97

Grant R F, Amrani M, Heaney D J, Wright R and Zhang M 2004a Mathematical modeling of phosphorus losses from land application of hog and cattle manure *J. Environ. Qual.* **33** 210–31

Grant R F, Arkebauer T J, Dobermann A, Hubbard K G, Schimelfenig T T, Suyker A E, Verma S B and Walters D T 2007a Net biome productivity of irrigated and rainfed maize-soybean rotations: Modeling vs. measurements *Agron. J.*

Grant R F and Baldocchi D D 1992 Energy transfer over crop canopies: simulation and experimental verification *Agric. For. Meteorol.* **61** 129–49

Grant R F, Baldocchi D D and Ma S 2012a Ecological controls on net ecosystem productivity of a seasonally dry annual grassland under current and future climates: Modelling with ecosys *Agric. For. Meteorol.* **152** 189–200

Grant R F, Barr A G, Black T A, Gaumont-Guay D, Iwashita H, Kidson J, McCaughey H, Morgenstern K, Murayama S, Nesic Z, Saigusa N, Shashkov A and Zha T 2007b Net ecosystem productivity of boreal jack pine stands regenerating from clearcutting under current and future climates *Glob. Chang. Biol.* **13** 1423–40

Grant R F, Barr A G, Black T A, Margolis H A, Dunn A L, Metsaranta J, Wang S, McCaughey J H and Bourque C A 2009a Interannual variation in net ecosystem productivity of Canadian forests as affected by regional weather patterns - A Fluxnet-Canada synthesis *Agric. For. Meteorol.* **149** 2022–39

Grant R F, Barr A G, Black T A, Margolis H A, Mccaughey J H and Trofymow J A 2010a Net ecosystem productivity of temperate and boreal forests after clearcutting-a FluxnetCanada measurement and modelling synthesis *Tellus, Ser. B Chem. Phys. Meteorol.* **62** 475–96

Grant R F, Black T A, Gaumont-Guay D, Klujn N, Barr A G, Morgenstern K and Nesic Z 2006a Net ecosystem productivity of boreal aspen forests under drought and climate change: Mathematical modelling with Ecosys *Agric. For. Meteorol.* **140** 152–70

Grant R F, Black T A, den Hartog G, Berry J A, Neumann H H, Blanken P D, Yang P C, Russell C and Nalder I A 1999a Diurnal and annual exchanges of mass and energy between an aspen-hazelnut forest and the atmosphere: Testing the mathematical model Ecosys with data from the BOREAS experiment *J. Geophys. Res.* **104** 27699–717

Grant R F, Black T A, Den Hartog G, Berry J A, Neumann H H, Blanken P D, Yang P C, Russell C and Nalder

I A 1999b Diurnal and annual exchanges of mass and energy between an aspen-hazelnut forest and the atmosphere: Testing the mathematical model Ecosys with data from the BOREAS experiment *J. Geophys. Res. Atmos.*

Grant R F, Black T A, Humphreys E R and Morgenstern K 2007c Changes in net ecosystem productivity with forest age following clearcutting of a coastal Douglas-fir forest: Testing a mathematical model with eddy covariance measurements along a forest chronosequence *Tree Physiol.* **27** 115–31

Grant R F, Black T A, Jassal R S and Bruemmer C 2010b Changes in net ecosystem productivity and greenhouse gas exchange with fertilization of Douglas fir: Mathematical modeling in ecosys *J. Geophys. Res. Biogeosciences* **115** 1–17

Grant R F, Desai A R and Sulman B N 2012b Modelling contrasting responses of wetland productivity to changes in water table depth *Biogeosciences* **9** 4215–31

Grant R F, Desai A R and Sulman B N 2012c Modelling contrasting responses of wetland productivity to changes in water table depth *Biogeosciences* **9** 4215–31

Grant R F and Flanagan L B 2007 Modeling stomatal and nonstomatal effects of water deficits on CO2 fixation in a semiarid grassland *J. Geophys. Res. Biogeosciences* **112** 1–16

Grant R F, Frederick, R J, Hesketh J D and Huck M G 1989 Maize Under Contrasting Water Regimesi *Can. J. Plant Sci.* **69** 401–18

Grant R F, Goulden M L, Wofsy S C and Berry J A 2001a Carbon and energy exchange by a black spruce-moss ecosystem under changing climate: Testing the mathematical model ecosyswith data from the BOREAS experiment *J. Geophys. Res.* **106** 33605–21 Online: http://www.agu.org/pubs/crossref/2001/2001JD900064.shtml%5Cnpapers2://publication/doi/10.1029/2001JD900064

Grant R F and Heaney D J 1997 Inorganic phosphorus transformation and transport in soils: Mathematical modeling in ecosys *Soil Sci. Soc. Am. J.* **61** 752–64

Grant R F, Humphreys E R and Lafleu P M 2015 Ecosystem CO2 and CH4 exchange in a mixed tundra and a fen within a hydrologically diverse Arctic landscape: 1. Modeling versus measurements *J. Geophys. Res.*

Biogeosciences **120** 1366–87

Grant R F, Humphreys E R, Lafleur P M and Dimitrov D D 2011a Ecological controls on net ecosystem productivity of a mesic arctic tundra under current and future climates *J. Geophys. Res. Biogeosciences* **116** 1–17

Grant R F, Hutyra L R, De Oliveira R C, Munger J W, Saleska S R and Wofsy S C 2009b Modeling the carbon balance of Amazonian rain forests: Resolving ecological controls on net ecosystem productivity *Ecol. Monogr.*

Grant R F, HUTYRA L R, OLIVEIRA R C DE, MUNGER J W, SALESKA S R and WOFSY S C 2009c Modeling the carbon balance of Amazonian rain forests : resolving ecological controls on net ecosystem productivity *Ecol. Modell.* **79** 445–63

Grant R F, Jarvis P G, Massheder J M, Hale S E, Moncrieff J B, Rayment M, Scott S L and Berry J A 2001b Controls on carbon and energy exchange by a black spruce-moss ecosystem: Testing the mathematical model Ecosys with data from the BOREAS Experiment *Global Biogeochem. Cycles*

Grant R F, Juma N G and McGill W B 1993a Simulation of carbon and nitrogen transformations in soil: Microbial biomass and metabolic products *Soil Biol. Biochem.* **25** 1331–8

Grant R F, Juma N G and McGill W B 1993b Simulation of carbon and nitrogen transformations in soil: Mineralization *Soil Biol. Biochem.* **25** 1317–29

Grant R F, Juma N G, Robertson J A, Izaurralde R C and McGill W B 2010c Long-Term Changes in Soil Carbon under Different Fertilizer, Manure, and Rotation *Soil Sci. Soc. Am. J.*

Grant R F, Kimball B A, Conley M M, White J W, Wall G W and Ottman M J 2011b Controlled warming effects on wheat growth and yield: Field measurements and modeling *Agron. J.*

Grant R F, Kimball B a, Pinter P J, Wall G W, Garcia R L, Lamorte R L and Hunsaker D J 1995 Carbon-Dioxide Effects on Crop Energy-Balance - Testing Ecosys with a Free-Air Co2 Enrichment (Face) Experiment *Agron. J.* **87** 446–57

Grant R F, Kimball B A, Wall G W, Triggs J M, Brooks T J, Pinter P J, Conley M M, Ottman M J, Lamorte R L, Leavitt S W, Thompson T L and Matthias A D 2004b Modeling elevated carbon dioxide effects on

water relations, water use, and growth of irrigated sorghum *Agron. J.*

Grant R F L B-2430 1991b The distribution of water and nitrogen in the soil-crop system: a simulation study with validation from a winter wheat field trial *Fertil. res.* **27** 199-213 ST-The distribution of water and nitrog

Grant R F, Margolis H A, Barr A G, Black T A, Dunn A L, Bernier P Y and Bergeron O 2009d Changes in net ecosystem productivity of boreal black spruce stands in response to changes in temperature at diurnal and seasonal time scales *Tree Physiol.*

Grant R F, Mekonnen Z A and Riley W J 2019a Modelling climate change impacts on an Arctic polygonal tundra. Part 1: Rates of permafrost thaw depend on changes in vegetation and drainage *J. Geophys. Res. Biogeosciences*

Grant R F, Mekonnen Z A, Riley W J, Arora B and Torn M S 2017a Mathematical Modelling of Arctic Polygonal Tundra with Ecosys: 2. Microtopography Determines How CO2 and CH4 Exchange Responds to Changes in Temperature and Precipitation *J. Geophys. Res. Biogeosciences* **122** 3174–87

Grant R F, Mekonnen Z A, Riley W J, Arora B and Torn M S 2019b Modelling climate change impacts on an Arctic polygonal tundra. Part 2: Changes in CO_2 and CH_4 exchange depend on rates of permafrost thaw as affected by changes in vegetation and drainage *J. Geophys. Res. Biogeosciences*

Grant R F, Mekonnen Z A, Riley W J, Arora B and Torn M S 2019c Modelling climate change impacts on an Arctic polygonal tundra. Part 2: Changes in CO_2 and CH_4 exchange depend on rates of permafrost thaw as affected by changes in vegetation and drainage *J. Geophys. Res. Biogeosciences* 2018JG004645 Online: https://onlinelibrary.wiley.com/doi/abs/10.1029/2018JG004645

Grant R F, Mekonnen Z A, Riley W J, Wainwright H M, Graham D and Torn M S 2017b Mathematical Modelling of Arctic Polygonal Tundra with Ecosys: 1. Microtopography Determines How Active Layer Depths Respond to Changes in Temperature and Precipitation *J. Geophys. Res. Biogeosciences* **122** 3161–73

Grant R F and Nalder I A 2000 Climate change effects on net carbon exchange of a Boreal aspen-hazelnut forest: Estimates from the ecosystem model ecosys *Glob. Chang. Biol.*

Grant R F, Neftel A and Calanca P 2016 Ecological controls on N2O emission in surface litter and near-surface soil of a managed grassland: Modelling and measurements *Biogeosciences*

Grant R F, Oechel W C and Ping C L 2003 Modelling carbon balances of coastal arctic tundra under changing climate *Glob. Chang. Biol.* **9** 16–36

Grant R F and Pattey E 2003 Estimating uncertainty in N 2 O emissions from U . S . cropland soils *Soil Biol. Biochem.* 225–43

Grant R F and Pattey E 1999 Mathematical modeling of nitrous oxide emissions from an agricultural field during spring thaw *Global Biogeochem. Cycles*

Grant R F and Pattey E 2008 Temperature sensitivity of N2O emissions from fertilized agricultural soils: Mathematical modeling in ecosys *Global Biogeochem. Cycles* **22** 1–10

Grant R F, Pattey E, Goddard T W, Kryzanowski L M and Puurveen H 2006b Modeling the Effects of Fertilizer Application Rate on Nitrous Oxide Emissions *Soil Sci. Soc. Am. J.* **70** 235 Online: https://www.soils.org/publications/sssaj/abstracts/70/1/235

Grant R F and Robertson J a 1997 Phosphorus uptake by root systems: mathematic modelling in ecosys *Plant Soil* **188** 279–97

Grant R F and Rochette P 1994 Soil microbial respiration at different water potentials and temperatures: theory and mathematical modeling *Soil Sci. Soc. Am. J.* **58** 1681–90

Grant R F and Roulet N T 2002 Methane efflux from boreal wetlands: Theory and testing of the ecosystem model Ecosys with chamber and tower flux measurements *Global Biogeochem. Cycles* **16** 2-1-2–16 Online: http://doi.wiley.com/10.1029/2001GB001702

Grant R F, Wall G W, Kimball B A, Frumau K F A, Pinter P J, Hunsaker D J and Lamorte R L 1999c Crop water relations under different CO2 and irrigation: Testing of ecosys with the free air CO2 enrichment (FACE) experiment *Agric. For. Meteorol.* **95** 27–51

Grant R F, Zhang Y, Yuan F, Wang S, Hanson P J, Gaumont-Guay D, Chen J, Black T A, Barr A, Baldocchi D D and Arain A 2006c Intercomparison of techniques to model water stress effects on CO2and energy exchange in temperate and boreal deciduous forests *Ecol. Modell.* **196** 289–312

Grant R, Kinch T, Bradley R, Whalen J K, Cogliastro A, Lange S F, Allaire S E and Parsons W F J 2017c Carbon Sequestration vs Agricultural Yields in Tree-Based Intercropping Systems as Affected by Tree Management *Can. J. Soil Sci.*

Grant S A and Sletten R S 2002 Calculating capillary pressures in frozen and ice-free soils below the melting temperature *Environ. Geol.* **42** 130–6

Krishnan P, Black T A, Barr A G, Grant N J, Gaumont-Guay D and Nesic Z 2008 Factors controlling the interannual variability in the carbon balance of a southern boreal black spruce forest *J. Geophys. Res. Atmos.*

Krishnan P, Black T A, Grant N J, Barr A G, Hogg E (Ted) H, Jassal R S and Morgenstern K 2006 Impact of changing soil moisture distribution on net ecosystem productivity of a boreal aspen forest during and following drought *Agric. For. Meteorol.*

Li T, Grant R F and Flanagan L B 2004 Climate impact on net ecosystem productivity of a semi-arid natural grassland: Modeling and measurement *Agric. For. Meteorol.* **126** 99–116

Manunta P, Grant R F, Feng Y, Kimball B A, Pinter P J, La Morte R L A, Hunsaker D J and Wall D J 2002 Changes in mass and energy transfer between the canopy and the atmosphere: Model development and testing with a free-air CO2 enrichment (FACE) experiment *Int. J. Biometeorol.* **46** 9–21

Mekonnen Z A, Grant R F and Schwalm C 2017 Carbon sources and sinks of North America as affected by major drought events during the past 30 years *Agric. For. Meteorol.*

Mekonnen Z A, Grant R F and Schwalm C 2016a Contrasting changes in gross primary productivity of different regions of North America as affected by warming in recent decades *Agric. For. Meteorol.*

Mekonnen Z A, Grant R F and Schwalm C 2018 Modelling impacts of recent warming on seasonal carbon exchange in higher latitudes of North America *Arct. Sci.*

Mekonnen Z A, Grant R F and Schwalm C 2016b Sensitivity of modeled NEP to climate forcing and soil at site and regional scales: Implications for upscaling ecosystem models *Ecol. Modell.*

Mezbahuddin M, Grant R F and Flanagan L B 2016 Modeling hydrological controls on variations in peat water content, water table depth, and surface energy exchange of a boreal western Canadian fen peatland *J.*

Geophys. Res. Biogeosciences

Mezbahuddin M, Grant R F and Hirano T 2015 How hydrology determines seasonal and interannual variations in water table depth, surface energy exchange, and water stress in a tropical peatland: Modeling versus measurements *J. Geophys. Res. Biogeosciences*

Schaefer K, Schwalm C R, Williams C, Arain M A, Barr A, Chen J M, Davis K J, Dimitrov D, Hilton T W, Hollinger D Y, Humphreys E, Poulter B, Raczka B M, Richardson A D, Sahoo A, Thornton P, Vargas R, Verbeeck H, Anderson R, Baker I, Black T A, Bolstad P, Chen J, Curtis P S, Desai A R, Dietze M, Dragoni D, Gough C, Grant R F, Gu L, Jain A, Kucharik C, Law B, Liu S, Lokipitiya E, Margolis H A, Matamala R, McCaughey J H, Monson R, Munger J W, Oechel W, Peng C, Price D T, Ricciuto D, Riley W J, Roulet N, Tian H, Tonitto C, Torn M, Weng E and Zhou X 2012 A model-data comparison of gross primary productivity: Results from the north American carbon program site synthesis *J. Geophys. Res. Biogeosciences*

Wang S, Grant R F, Verseghy D L and Black T A 2001 Modelling plant carbon and nitrogen dynamics of a boreal aspen forest in CLASS - The Canadian Land Surface Scheme *Ecol. Modell.*

Wang Z, Grant R F, Arain M A, Bernier P Y, Chen J M, Govind A, Guindon L, Kurz W A, Peng C, Price D T, Stinson G, Sun J, Trofymowe J A and Yeluripati J 2013 Incorporating weather sensitivity in inventory-based estimates of boreal forest productivity: A meta-analysis of process model results *Ecol. Modell.*

Wang Z, Grant R F, Arain M A, Chen B N, Coops N, Hember R, Kurz W A, Price D T, Stinson G, Trofymow J A, Yeluripati J and Chen Z 2011 Evaluating weather effects on interannual variation in net ecosystem productivity of a coastal temperate forest landscape: A model intercomparison *Ecol. Modell.*

Zhang Y, Grant R F, Flanagan L B, Wang S and Verseghy D L 2005 Modelling CO 2 and energy exchanges in a northern semiarid grassland using the carbon- and nitrogen-coupled Canadian Land Surface Scheme (C-CLASS) *Ecol. Modell.*